Spontaneous magnetic moments in clean normal-metal–superconductor proximity layers

Felix Niederer, Alban L. Fauchère, and Gianni Blatter
Theoretische Physik, Eidgenössische Technische Hochschule, CH-8093 Zürich, Switzerland
(Received 26 April 2001; published 26 March 2002)

We investigate the spontaneous paramagnetic moments in clean normal-metal–superconductor proximity layers caused by the π-state currents that arise at the interface if a repulsive electron-electron interaction is assumed in the normal metal. Accounting for the nonlocal current response characteristic of the clean limit, we present a self-consistent numerical solution of the coupled Eilenberger and Maxwell equations in the limits of small and large electron densities, the latter giving rise to an internal magnetic breakdown. Comparison with experiment allows us to estimate the normal-metal coupling constant.

DOI: 10.1103/PhysRevB.65.132515 PACS number(s): 74.50.+r, 75.20.−g

The low-temperature magnetic screening in a thin normal-metal layer (N) in contact with a bulk superconductor (S) is governed by the proximity effect: The Andreev reflection of the normal-metal quasiparticles at the NS interface allows the superconductor to export its coherent state into the metallic layer. At temperatures below the Andreev energy $k_B T_A = \hbar v_F / 2\pi d$ (d denotes the thickness of the normal-metal layer), the induced superconductivity produces a diamagnetic response: accounting for nonlocal screening in the clean limit, the quasiclassical Eilenberger theory predicts a large diamagnetic susceptibility[1] $4\pi\chi = -3/4$ at $T \ll T_A$. This proximity-induced diamagnetism is quite susceptible to temperature and field: (i) at high temperatures $T \gg T_A$ screening is exponentially suppressed,[1] $\chi(T \gg T_A) \propto \exp(-2T/T_A)$; (ii) at large applied fields the induced supercurrents become mutually dephased and the proximity effect breaks down in a first-order phase transition at the breakdown field[2,3] $H_b(T=0) \approx \Phi_0/6d\lambda$. The theoretical results in the ballistic regime with a mean free path $l \sim d$ are in good quantitative agreement with the measured susceptibility for superconducting cylinders coated with a normal metal.[4]

At ultralow temperatures, however, a paramagnetic reentrance in the susceptibility has been observed,[5] which disagrees with the conventional understanding of the proximity effect and has spurred much theoretical attention.[6–8] Recently, the implications on the transverse screening due to a repulsive electron-electron interaction in the normal-metal have been investigated:[9] In addition to the linear suppression $N(E) \sim N_0 E d/\hbar v_F$ ($N_0 = m k_F/\hbar^2\pi^2$) of the density of states (DOS) close to the Fermi level due to the Andreev bound states,[10] a zero-energy DOS with macroscopic weight has been shown to appear at the interface of the two metals. In the presence of a magnetic field the DOS peak splits and induces, at sufficiently low temperatures, spontaneous paramagnetic currents $j_{\rm para}$ along the SN interface, superimposed on the usual screening currents $j_{\rm dia}$. Fauchère *et al.*[9] proposed this sizable paramagnetic response as a possible explanation of the reentrance effect observed in the experiments by Mota and co-workers.[5] Formation of such zero-energy states is known from other superconducting systems, such as SNS Josephson junctions biased with a phase difference π and (110) d-wave superconductors producing spontaneous surface currents.[11,12]

In the discussion presented in Ref. 9 the order parameter Δ within the normal layer has been approximated by a constant and the nonlocal character of proximity screening has been neglected. In this paper we improve upon this situation and present a self-consistent numerical solution for the coupled Eilenberger and Maxwell equations describing the superconducting and nonlocal electromagnetic response of the SN proximity system. We find that the non-local current response enhances the effect of a normal-metal electron-electron interaction on the proximity superconductivity as compared with the approximate local model.[9] We discuss the nontrivial current distribution resulting from overscreening and investigate the possibility of an internal magnetic breakdown triggered by a large spontaneous magnetic moment. Comparing our results with experiments, we arrive at an estimate for the repulsive coupling V_N required to produce the observed paramagnetic signal.

We briefly review the proximity-induced superconductivity in clean NS layers as presented in Refs. 2, 3, and 9. We first concentrate on the simpler situation with noninteracting electrons in the normal-metal layer, and discuss the first-order-type diamagnetic to paramagnetic transition induced by a large magnetic field. At low temperatures $T \ll T_A$ an applied magnetic field H is diamagnetically screened in the linear response. Nonlocality, a characteristic of the clean limit, manifests itself through a spatially constant screening current within the normal-metal layer N, leading to an *overscreening*[1] of the applied field H with a reversed magnetic field $-H/2$ at the SN interface; as a consequence, the Meissner susceptibility is reduced to a value $4\pi\chi = -3/4$. At large fields a magnetic breakdown[3] occurs as the induced supercurrents are mutually dephased by the large magnetic field—as a result, the diamagnetic screening capability is lost and the normal-metal layer turns paramagnetic. At low temperatures the two resulting phases are thermodynamically separated by a first-order phase transition[2,3] exhibiting a jump of the magnetization of the NS system at the breakdown field $H_b \sim \Phi_0/\lambda d$. The two phases coexist as metastable solutions between the supercooled and the superheated spinodals, $H_{\rm sc} \sim \Phi_0/d^2$, $H_{\rm sh} \sim \Phi_0/\lambda^2$, respectively.

Next, we include a repulsive electron-electron interaction in the normal-metal layer N; as shown in Ref. 9 this leads to a paramagnetic instability at sufficiently low temperatures. The proximity-induced superconductivity originates from bound electron-hole states, where electrons and holes are transformed into each other via Andreev reflection at the NS interface. In the usual interaction-free, i.e., free-electron gas,

description, the Andreev bound states are found at energies $E_n=\hbar v_x(2n+1)\pi/4d$ $(n=0,1,\ldots;v_x=v_F\cos\theta)$, resulting in a linear suppression $N(E)\sim N_0Ed/\hbar v_F$ of the DOS close to the Fermi energy $E=0$. A finite positive normal-metal coupling constant $V_N>0$ induces a finite order parameter $\Delta(x)$ in the normal-metal layer with a sign opposite to the value in the bulk superconductor. As a consequence, the Andreev energy levels are shifted and the local DOS at the interface exhibits an additional pronounced peak at zero energy. The magnetic behavior of the proximity layer is very susceptible to such a deformation of the DOS: besides the (nonlocal) diamagnetic response $j_{\rm dia}$, an additional paramagnetic component $j_{\rm para}$ appears close to the NS interface due to the finite DOS at the Fermi level; under suitable conditions the peak in the DOS is strong enough to induce a paramagnetic instability as the free energy $\delta F=-cj\,\delta A<0$ can be lowered by a nonzero magnetic induction evoked by a spontaneous current flow along the NS interface.

In a third step we can combine the two phenomena discussed above: if the paramagnetic instability is weak, the resulting magnetic induction cannot dephase the Andreev states and the two phenomena of paramagnetic instability and magnetic breakdown will remain well separated. On the other hand, the field of a strong paramagnetic instability may join with the external magnetic field and induce an ''inner'' magnetic breakdown of the diamagnetic screening in the *N* layer. In the following, we present a detailed description of our numerical calculation of the magnetic properties of a clean NS proximity system and discuss two situations involving a weak and a strong paramagnetic instability.

The cylindrical samples produced by Mota and coworkers[5] and exhibiting the reentrant effect consist of a Nb core of radius $r\approx 10$ μm with a coherence length $\xi_S^0=\hbar v_F/\pi\Delta_S\approx 40$ nm; the superconducting core is coated by a Ag layer of thickness $d\approx 3$ μm, with an interface of high transparency,[13] while the mean free path l of the normal metal is of the order of the normal-layer thickness *d*. Given the electron density of Ag, the London length $\lambda=22$ nm of the normal metal is small compared to the geometrical dimensions $\lambda/d\approx 1/150$.

Neglecting the cylindrical geometry, we describe the proximity system by a clean normal-metal slab of thickness *d* $(0<x<d)$ in contact with a bulk superconductor $(x<0)$. The SN-interface is assumed to be perfectly transparent: although the linear paramagnetic response is sensitive[14] to a finite interface reflectivity *R*, the nonlinear paramagnetic current survives a sufficiently small imperfection of order $R\sim 0.1$, as shown numerically by Belzig.[15]

We express the magnetic induction $B_z(x)[\equiv B(x)]$ by the potential $A_y(x)[\equiv A(x)]$ and solve the self-consistency loop below. The 2×2 matrix Green's function $\hat{g}(x,\mathbf{v}_F)$ follows from the Eilenberger equation

$$-\hbar v_x\partial_x\hat{g}=[\{\hbar\omega+(ie/c)v_yA(x)\}\hat{\tau}_3+\Delta(x)\hat{\tau}_1,\hat{g}], \quad (1)$$

together with the self-consistency equation for the pair potential

$$\Delta(x)=-VN_0\pi T\sum_{\omega>0}\langle f_\omega(x,\mathbf{v}_F)\rangle. \quad (2)$$

Here, $\hat{\tau}_i$ are the Pauli matrices and $\hat{g}$ contains the Green's functions $g_\omega(x,\mathbf{v}_F)$ and $f_\omega(x,\mathbf{v}_F)$, which depend on the Matsubara frequency $\omega=\pi T(2n+1)$ and the direction of the Fermi velocity $\mathbf{v}_F$. $N_0=mk_F/\hbar^2\pi^2$ is the DOS at the Fermi level and $\langle\cdots\rangle$ denotes angular averaging over the Fermi sphere. The Green's function $g_\omega(x,\mathbf{v}_F)$ determines the current-field relation $j[A]$ $(j\equiv j_y)$,

$$j(x)=ieN_0 2\pi T\sum_{\omega>0}\langle v_y g_\omega(x,\mathbf{v}_F)\rangle. \quad (3)$$

Finally, in order to find the vector potential *A* and the current *j* for a given applied magnetic field *H*, the set of Eqs. (1)–(3) has to be solved self-consistently together with Maxwell's equation $j(x)=-(c/4\pi)\partial_x^2A(x)$, respecting the boundary conditions $A|_{-\infty}=0$ and $\partial_xA|_d=H$. The vector potential then is inserted back into the Eilenberger Eq. (1), thus closing the self-consistency loop. The coupling constants $V_S<0$ and $V_N>0$ in the two metals enter the quasiclassical description via the self-consistency Eq. (2) for the pair potential. Assuming a perfect transparency at the SN interface the Green's function $\hat{g}$ is continuous at $x=0$, while at the vacuum boundary $x=d$ we demand specular reflection of the quasiparticle trajectories, $\hat{g}_\omega(d,v_x,v_y)=\hat{g}_\omega(d,-v_x,v_y)$.

Solving the self-consistency problem outlined above numerically,[16] we calculate the magnetization

$$4\pi M(H)=\frac{1}{d}\left[\int_{-\infty}^{d}dx(B(x)-H)-\int_{-\infty}^{0}dx(He^{x/\lambda}-H)\right] \quad (4)$$

$$\equiv 4\pi\mathcal{M}-H\lambda/d, \quad (5)$$

where, for convenience, we compare the magnetization of the proximity system (S: $x<0$, N: $0<x<d$) to that of a superconductor (S: $x<0$). In order to decide on the thermodynamic stability of the solution we compute the Gibbs free-energy density $\mathcal{G}(H)=\mathcal{F}(\mathcal{M})-\mathcal{M}H$ including the kinetic energy of the supercurrents $j(x)=-\delta\mathcal{F}/\delta A(x)$ and the electromagnetic field energy $B^2/8\pi$, hence

$$\mathcal{F}(\mathcal{M})=-\frac{1}{cd}\int_{-\infty}^{d}dx\int_0^A dA'(x)j[A'(x)]$$
$$+\frac{1}{8\pi d}\int_{-\infty}^{d}dxB^2(x)-\frac{H^2}{8\pi};$$

the field dependence of the condensation energy density $N_0\Delta(x)^2/2$ and of the energy cost of a finite gap $\Delta(x)$ in the normal metal turn out to be negligible.

The results for the self-consistent screening problem we present below are based on a moderate normal-metal coupling constant $V_NN_0\leqslant 0.1$, while for the superconductor we adopt the standard value for Nb, $V_SN_0=-0.31$. We find that the magnetization curve $M(H)$ depends strongly on the elec-

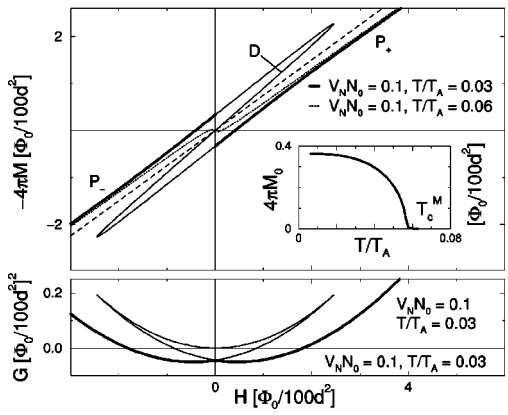

FIG. 1. *Above:* Magnetization curves $M(H)$ below (solid line) and above (dotted line) the critical temperature $T_c^M=0.06T_A$ for $\lambda=100$ nm, $d=1$ μm, $V_N N_0=0.1$. For comparison we show the Meissner screening curve $-4\pi M=3H/4$ of the interaction-free case (dashed line). The thick line indicates the thermodynamically stable solution possessing the lowest Gibbs free energy (*below*). *Inset:* temperature dependence of the spontaneous zero-field magnetization $M_0(T,H=0)$.

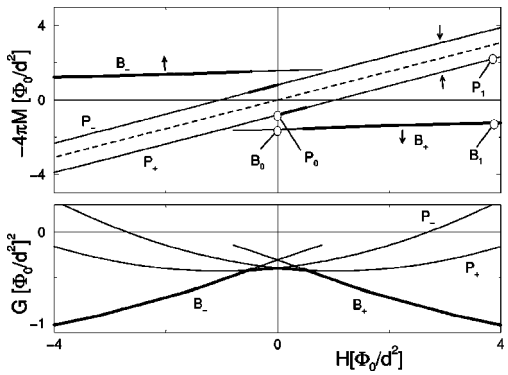

FIG. 2. Magnetization curve $M(H)$ and Gibbs free energy $\mathcal{G}(H)$ for $\lambda\approx 20$ nm, $d\approx 1$ μm, $V_N N_0=0.1$, and $T=1.25\,T_A$. The two screening branches $P\pm$ with diamagnetic slope $4\pi\chi=-3/4$ exhibit a paramagnetic offset M_0 produced by the π-state currents. The breakdown branches $B_\pm$ extend to external fields H of opposite sign. The arrows indicate the polarization of the π-state currents ($\downarrow\hat{=}j_{\rm para}>0$), the dashed line $4\pi M=-3H/4$ is a guide to the eyes.

tron density via the London length λ. For illustrative purposes we discuss our results in two opposite limits.

(i) For a large (as compared to the value in Ag) London length $\lambda\approx 100$ nm the spontaneous magnetization created by the π-state currents is small as compared to the breakdown field $H_b\sim\Phi_0/d\lambda$ (and even with respect to the lower spinodal $H_{\rm sc}\sim\Phi_0/d^2$, see Ref. 3). The magnetic signal due to the paramagnetic currents then is well separated from that due to the magnetic breakdown and the qualitative predictions of Ref. 9 are well confirmed.

(ii) A large electron density (implying a small London length λ close to the value in Ag) enhances the effect of the repulsive interaction; the spontaneous paramagnetic currents become large and eventually trigger an internal magnetic breakdown, changing the magnetization curve $M(H)$ in a qualitative way.

The magnetization for case (i) with a large London parameter $\lambda\approx 100$ nm and a normal-metal length $d\approx 1$ μm is shown in Fig. 1. Below the critical temperature $T_c^M=0.06\,T_A$ the magnetization curve $M(H)$ splits into a linear screening branch D with enhanced slope $-4\pi\chi>3/4$ and two screening branches $P_\pm$ shifted by a paramagnetic magnetization M_0 and exhibiting the usual clean-limit Meissner susceptibility $-4\pi\chi=3/4$ as in the interaction-free case (dashed line). The Gibbs free-energy density of the solutions $P_\pm$ is reduced by $\delta E\approx -Aj_{\rm para}$ and hence they represent the thermodynamically stable branches, while the linear branch D has turned unstable. The spontaneous magnetization $M_0(T)$ saturates at low temperatures and collapses on approaching the critical value T_c^M, see inset. Above T_c^M the spontaneous magnetization vanishes and the solution becomes single valued (dotted line). All these features are in qualitative accordance with the predictions of the local model;[9] still, we note that the paramagnetic currents at the interface are reversed and overscreened due to the nonlocal screening, an effect discussed in more detail below.

For this large London length λ the zero-field magnetization M_0 and the pair potential $\Delta_N(x=0)$ scale linearly with the coupling V_N. For the parameters chosen here the spontaneous magnetization is small compared to the lower spinodal field $H_{\rm sc}=\Phi_0/d^2$ of the magnetic breakdown,[3] $M_0\ll H_{\rm sc}<H_b$, and thus the appearance of paramagnetic currents at small fields is well separated from the breakdown regime at large fields.

Second, we turn to the opposite limit of large electron densities, i.e., small penetration depth $\lambda\approx 20$ nm. The effect of the π-state currents then is large and the induced screening behavior deviates qualitatively from the simple description of Ref. 9. In Fig. 2 we show the magnetization curve at $T=1.25T_A$ of the order of the Andreev energy. The two screening branches $P_\pm$ still possess a diamagnetic slope $4\pi\chi=-3/4$ due to nonlocal screening and exhibit a paramagnetic offset M_0. In addition, a second branch $B_\pm$ extends down to low fields where the induced superconductivity has broken down. This branch describes a penetrating field solution with fluxes $\Phi=\int_{-\infty}^{d}dxA(x)>\Phi_0$ large enough to dephase the induced screening currents. This breakdown solution is limited to fields $|H|>\Phi_0/d^2=H_{\rm sc}$ in the interaction-free case; here, the paramagnetic interface currents are large enough to trigger an 'internal' breakdown extending down to zero fields.

The field $(A(x),B(x))$ and current $[j(x)]$ configurations are shown in Fig. 3. The field configurations for the zero-field screening solution P_0 and for a generic point P_1 on the screening branch P_+ illustrate the nonlocal character of the Meissner screening in the clean limit: the orientation of the π-state currents producing the paramagnetic offset is determined by the direction of the field at the interface, which is reversed with respect to the external field due to over screening; hence the paramagnetic current flows in a direction *opposite* to what is expected within a local theory. The large magnetic induction $B(x)$ at the SN interface caused by the π-state currents then is in turn overscreened by the induced Meissner currents, reversing the net effect of the spontaneous

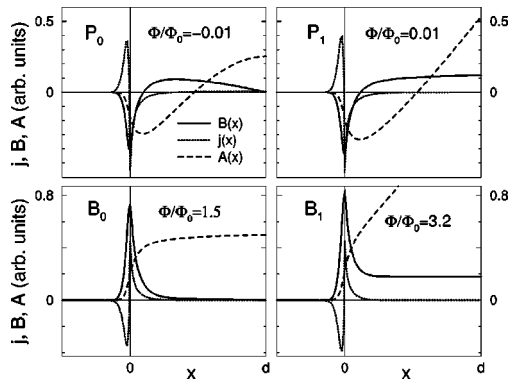

FIG. 3. Current density $j(x)$, magnetic induction $B(x)$, and vector potential $A(x)$ for the two screening solutions P_0 and P_1 and the two penetrating field solutions B_0 and B_1. The peak in the magnetic field B at the interface is (over)screened for P_0 and P_1, while the screening currents have broken down for configurations B_0 and B_1.

currents on the magnetization M and producing a net paramagnetic signal. Note that the shape of the vector potential $A(x)$ efficiently keeps the flux $|\Phi|=|\int dxA|$ below the flux quantum Φ_0. The field configurations for the breakdown solutions $B_{0,1}$, on the other hand, explain why the initiation of the breakdown is moved to lower fields: The π-state currents are oriented such that their magnetic moments M_0 are aligned with the applied field H and further augment the flux Φ (see the field configuration B_1 shown in Fig. 3). As a consequence, dephasing of the screening currents is enhanced and the breakdown branches $B_{\pm}$ extend to lower applied fields $|H|<H_{sc}$. For the (extreme) parameters chosen here, $B_{\pm}$ cross the $H=0$ axis, allowing for the zero-field *internal breakdown* solution B_0 shown in Fig. 3.

The scaling of the screened zero-field magnetization $M_0(V_N)$ is shown in Fig. 4 for a layer thickness $d \approx 3.5$ μm approximating the experimental sample. In contrast to our results for large values of λ where $M_0 \propto V_N$ scales linearly with V_N, at high electron densities the spontaneous currents produce a magnetization M_0 depending logarithmically on the interaction V_N, although the interface value $\Delta_N(0)$ still scales linearly with V_N.

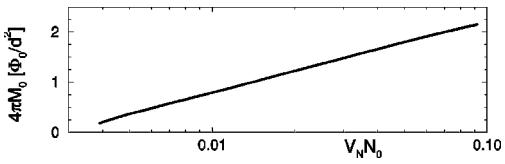

FIG. 4. Zero-field magnetization of the screening solution as a function of the coupling constant V_N. For $\lambda \approx 20$ nm, $d \approx 3.5$ μm, $T=1.75T_A$, and $V_S N_0=-0.31$ the magnetization $M_0 \propto \ln(V_N)$ scaled logarithmically with V_N.

Müller-Allinger and Mota[17] have measured a dc magnetization curve $M(H)$ exhibiting an offset of the order of $M(H=0)\approx 1$ Gauss ($\Phi_0/d^2=1.9$ Gauss for sample 5AgNb in Ref. 17). Hence even a small normal-metal coupling constant $V_N N_0 \approx 0.008 \ll |V_S| N_0$ is enough to explain the experimentally observed paramagnetic reentrance, see Fig. 4. Note that such a small negative value for the effective coupling constant $V_N N_0 \approx \lambda_{ph} - \mu^*$ is compatible with estimates[18] for the dimensionless electron-phonon coupling $\lambda_{ph} \approx 0.13 \pm 0.04$ in Ag and typical values $\mu^* \approx 0.1$–0.2 for the repulsive Coulomb interaction parameter.

In summary, we have calculated the induced Meissner screening for a clean SN proximity system, assuming a finite repulsive coupling constant in the normal metal. The sign change in the order parameter across the SN interface produces a zero-energy DOS peak leading to the formation of spontaneous magnetic moments at low temperatures. This instability persists in the presence of nonlocal screening characteristic of the clean limit. Indeed, the induced paramagnetic moments may even be large enough to trigger an internal breakdown of proximity screening. For lengths d and λ comparable to experiment (e.g., sample 5AgNb in Ref. 17) we find that a small coupling $V_N N_0 \sim 0.01$ is already sufficient to produce a zero-field magnetization M_0 of the order of the experimentally measured offset in the diamagnetic magnetization curve $M(H)=-\chi H \pm M_0$.

We wish to thank A. C. Mota and B. Müller-Allinger for discussions and acknowledge W. Belzig and R. Monnier for fruitful comments.

[1] A.D. Zaikin, Solid State Commun. **41**, 533 (1982).
[2] W. Belzig *et al.*, Phys. Rev. B **53**, 5727 (1996).
[3] A.L. Fauchère and G. Blatter, Phys. Rev. B **56**, 14 102 (1997).
[4] F.B. Müller-Allinger *et al.*, Phys. Rev. B **59**, 8887 (1999).
[5] P. Visani, A.C. Mota, and A. Pollini, Phys. Rev. Lett. **65**, 1514 (1990); A. C. Mota *et al.*, Physica B **197**, 95 (1994).
[6] W. Belzig, C. Bruder, and A.L. Fauchère, Phys. Rev. B **58**, 14 531 (1998).
[7] C. Bruder and Y. Imry, Phys. Rev. Lett. **80**, 5782 (1998).
[8] A.L. Fauchère, V. Geshkenbein, and G. Blatter, Phys. Rev. Lett. **82**, 1796 (1999); C. Bruder and Y. Imry, *ibid.* **82**, 1797 (1999).
[9] A.L. Fauchère, W. Belzig, and G. Blatter, Phys. Rev. Lett. **82**, 3336 (1999).
[10] P.G. de Gennes, Rev. Mod. Phys. **36**, 225 (1964).
[11] Chia-Ren Hu, Phys. Rev. Lett. **72**, 1526 (1994).
[12] M. Matsumoto and H. Shiba, J. Phys. Soc. Jpn. **64**, 1703 (1995).
[13] A good (microscopic) quality of the interface has been inferred from the analysis of the breakdown field, see A.C. Mota, P. Visani, and A. Pollini, J. Low Temp. Phys. **76**, 465 (1989); **76**, 508 (1989).
[14] A. Shelankov and M. Ozana, Phys. Rev. B **61**, 7077 (2000).
[15] W. Belzig, Physica B **284**, 1890 (2000).
[16] Before integration we transform Eq. (1) to a decoupled set of Riccati equations, see N. Schopohl and K. Maki, Phys. Rev. B **52**, 490 (1995).
[17] F.B. Müller-Allinger and A.C. Mota, Phys. Rev. Lett. **84**, 3161 (2000).
[18] G. Grimvall, *The Electron-Phonon Interaction in Metals* (North Holland, Amsterdam, 1981), p. 256.